Nodes versus Minima in the Energy Gap of Iron Pnictide Superconductors from Field-Induced Anisotropy

A. B. Vorontsov
Department of Physics, Montana State University, Bozeman, Montana, 59717, USA

I. Vekhter
Department of Physics and Astronomy, Louisiana State University, Baton Rouge, Louisiana, 70803, USA
(Received 20 May 2010; published 28 October 2010)

We develop the formalism for computing the oscillations of the specific heat and thermal transport under rotated magnetic field in multiband superconductors with anisotropic gap and apply it to iron-based materials. We show that these oscillations change sign at low temperatures and fields, which strongly influences the experimental conclusions about the gap structure. We find that recent measurements of the specific heat oscillations indicate that the iron-based superconductors possess an anisotropic gap with deep minima or nodes close to the line connecting electron and hole pockets. We predict the behavior of the thermal conductivity that will help distinguish between these cases.

DOI: 10.1103/PhysRevLett.105.187004 PACS numbers: 74.20.Rp, 74.25.fc, 74.70.Xa

Discovery of superconductivity in iron pnictides reenergized the effort to understand the properties of the paired state in correlated electron systems. Materials containing FeAs [1,2] or Fe(Se,S,Te) [3,4] layers are quasi-two-dimensional, and most are antiferromagnetic (AFM) at stoichiometry, which led to early comparisons to the cuprate superconductors (SCs). Unlike cuprates, the pnictides remain metallic [1–7] in the AFM state, suggesting that the itinerant correlated picture is more appropriate. This view is also supported by the agreement between the band structure calculations and the measured Fermi surface [8–12].

The complication is that all five d orbitals of Fe ions contribute to the density of states (DOS) close to the Fermi level resulting in multiple Fermi surface (FS) sheets. The complete description of these materials includes two to three hole bands at the center (Γ point) of the Brillouin zone (BZ) and two electron bands in the corner of the BZ, hereafter referred to as M point. This multiband nature is essential for the ongoing debate about the structure of the superconducting order parameter in iron-based SCs.

Superconductivity in pnictides is likely due to the magnetically assisted electron scattering between the nearly-nested hole (h) and electron (e) FS sheets [8], leading to a so-called $s^{\pm}$ state, with both pockets fully gapped, and $\Delta_e = -\Delta_h$ [13–15]. Detailed description of spin fluctuations and intraband Coulomb scattering favors anisotropic gaps: only on the electron sheets for the A_{1g} (extended s-wave) representation, [16–20], and on all FS sheets for the gap of B_{1g} (d-wave) character [21,22]. The latter gap shape is unlikely since ARPES measurements see nearly uniform gaps on h FS [10,23–28].

The magnitude of the anisotropic component in the A_{1g} state depends on the values of the interaction parameters and hence is material dependent. Thus, possibilities range from isotropic Δ_e, to a gap with deep minima on the e FS along Γ-M line, to a state with a pair of *"accidental"* nodes near this line [18,19,29]. In the unlikely case of the dominant anisotropic component, the nodes move to positions along the sides of the crystallographic BZ. Signatures of low-energy excitations were found in Co-doped $Ba(FeAs)_2$ [30], LaFePO [31,32], $BaFe_2(As_{1-x}P_x)_2$ [33–35] and Fe(Se,Te) [36] materials. However, the detailed gap structure of the pnictides, including the location of the possible nodes on the electron sheet, still needs to be unambiguously determined.

Oscillations of the thermodynamic and transport coefficients in SCs with anisotropic gap as a function of the relative orientation of the magnetic field and the nodal (or quasinodal) directions [37–41] are extensively used to determine the position of the *symmetry-enforced* gap nodes [42,43]. The key prediction of the inversion of the anisotropy [39], the switch from the minima to maxima for the field along the direction of the smallest gap, was recently confirmed [44]. A similar test was suggested for pnictides in Ref. [45], and very recent measurements of the specific heat in the vortex state of Fe(Se,Te) [46] were interpreted as leading to a surprising conclusion that the nodes of the gap are along the principal directions in the Brillouin zone. This stimulated our study.

In this Letter we develop the formalism for computing the properties of the vortex state of multiband two-dimensional (2D) superconductors under an in-plane magnetic field. We specifically address the states without symmetry-enforced nodes, such as pnictides. [47] We analyze the behavior of the specific heat, (C), and the electronic thermal conductivity, (κ), focusing on the regime where the inversion of the oscillations occurs, and compare it with data in Ref. [46]. Accounting for the inversion we find that, contrary to the conclusions of that paper, the results are most consistent with either deep minima

or nodes close to the Γ-M direction. We predict the evolution of the C and κ as a function of the field direction for different temperatures and fields.

We consider a superconducting gap with the basis function in the A_{1g} representation, $\mathcal{Y}(k_x, k_y) = a + b(\cos k_x + \cos k_y)$, where k_x and k_y belong to the unfolded Brillouin zone, Fig. 1(a), and the ratio a/b determines the anisotropy of the gap. In that scheme a circular hole sheet is centered around Γ point, and the electron sheets are centered around M point and its equivalents. This $\mathcal{Y}(k_x, k_y)$ gives nearly isotropic order parameter on the h FS, $\Delta_h(\phi) = \Delta_1$, and, generally, an anisotropic gap on the e FS, $\Delta_e(\phi) = \Delta_2 \mathcal{Y}_e(\phi)$,

$$\mathcal{Y}_e(\phi) = (1 - r) \mp r \sin 2\phi, \qquad \mp \quad \text{for } M, M', \quad (1)$$

where ϕ is the angle from the [100] direction, see Fig. 1. The gap has either minima along Γ-M line [$r < 0.5$, Fig. 1(a)] or nodes close to Γ-M line for $r \gtrsim 0.5$, which approach [100] and [010] directions for $r = 1$, Fig. 1(b).

We compute the field-dependent specific heat and electronic thermal conductivity by solving the equation for the quasiclassical Green's function $\hat{g}$ in the particle-hole (Nambu) space, as in Refs. [40,41]. To treat multiple bands we introduce $\hat{g}_{n=1,2}(\mathbf{R}, k; \varepsilon)$, with k parameter running over the hole FS ($n = 1$) twice (two equivalent hole bands), and over the two electronic FSs ($n = 2$) at points M and M'. In each band, given the Fermi velocity $\mathbf{v}_n(k)$ and the vector potential $\mathbf{A}(\mathbf{R})$ of the magnetic field, we solve the transport equation for $\hat{g}_n$ at energy ε,

$$\left[\left(\varepsilon + \frac{e}{c}\mathbf{v}_n \mathbf{A}(\mathbf{R})\right)\hat{\tau}_3 - \hat{\Delta}_n - \hat{\sigma}_n, \hat{g}_n\right] + i\mathbf{v}_n \cdot \boldsymbol{\nabla}_{\mathbf{R}} \hat{g}_n = 0, \quad (2)$$

subject to the normalization condition $\hat{g}_n^2 = -\pi^2 \hat{1}$. Here $\hat{\tau}_3$ is the Pauli matrix, and the spatial dependence of the order parameter is that of the Abrikosov vortex lattice,

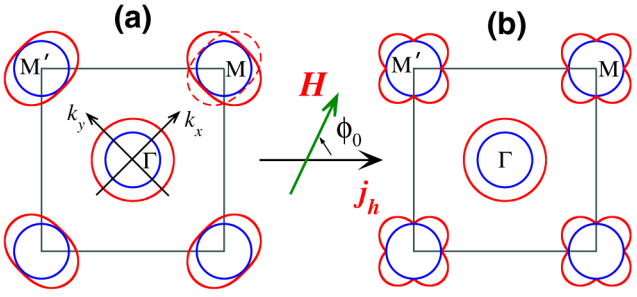

FIG. 1 (color online). Fermi surfaces and energy gaps in the two-band model of iron pnictides. The true structure is obtained by folding the FS sheets (blue [dark gray]) and SC gaps (red [medium gray]) along the sides of the square (full and dashed lines at M). The hole FS around Γ has an isotropic gap. The A_{1g} gap on the electronic FS may be isotropic, have deep minima along Γ-M line [panel (a), $r = 0.45$ in Eq. (1)] or nodes along the [100] as in panel (b), $r = 1$. We take the heat current along [100], as shown.

$$\Delta_n(\mathbf{R}, k) = \Delta_n(k) \sum_{l_y} C_{l_y} \frac{e^{i l_y \tilde{y}}}{\sqrt{\Lambda}} \tilde{\Phi}_0\left(\frac{\tilde{x} - \Lambda^2 l_y}{\Lambda}\right),$$

where $\tilde{\Phi}_0(z)$ is the ground state wave function of a harmonic oscillator, $\tilde{x}$ and $\tilde{y}$ are in the plane normal to the field, and the magnetic length $\Lambda^2 = \hbar c/2eH$. Two bands are mixed through the self-consistency on $\Delta_n(\mathbf{R}, k) = T\sum_{\varepsilon_m, k', n'} V_{n,n'}(k, k') f_{n'}(\mathbf{R}, k'; \varepsilon_m)$, where f_n, the Gorkov pairing amplitude, is the off-diagonal component of $\hat{g}_n$, and on the impurity self-energy, $\hat{\sigma}_n$, which is determined in the self-consistent t-matrix approximation for two bands [48], so that $\hat{\sigma}(\mathbf{R}; \varepsilon) = n_{\text{imp}} \hat{t}_s(\mathbf{R}; \varepsilon)$. We take a negative interband pair hopping, $V_{12}(k, k') = -|V| \mathcal{Y}(k) \mathcal{Y}(k')$ which leads to the opposite signs of gaps Δ_1 and Δ_2.

We employ the extended Brandt-Pesch-Tewordt (BPT) approximation where the diagonal components of $\hat{g}_n$, the propagators g_n and $\bar{g}_n$, are replaced by their spatial average, while the full dependence of f_n is kept. This approach is described and justified in Refs. [40,49,50], and the results obtained from the self-consistent solution of the quasiclassical equations in a single band agree with those obtained using our method nearly perfectly. [51]

Once the Green's function and the self-energies are determined, we find the low-temperature specific heat from

$$\frac{C(T, \mathbf{H})}{T} = \int_{-\infty}^{\infty} \frac{d\varepsilon}{T} \frac{\varepsilon^2}{4T^2} \cosh^{-2} \frac{\varepsilon}{2T} \sum_{n=1,2} N_n(\varepsilon, T, \mathbf{H}), \quad (3)$$

where $N_n(\varepsilon, T, \mathbf{H}) = -\frac{1}{\pi}\langle \Im \mathrm{m} g_n(\varepsilon, k)\rangle_{\text{FS}}$, is the DOS in each band and the angular brackets denote averaging over the corresponding FS. Similarly, $\kappa_{xx} = \kappa_{1,xx} + \kappa_{2,xx}$, where each Fermi surface contributes

$$\frac{\kappa_{n,xx}}{T} = \int_{-\infty}^{+\infty} \frac{d\varepsilon}{T} \frac{\varepsilon^2}{2T^2} \cosh^{-2} \frac{\varepsilon}{2T} \times \langle v_{n,x}^2 N_n(T, \boldsymbol{H}; k, \varepsilon) \tau_{H,n}(T, H; k,)\rangle_{\text{FS}}, \quad (4)$$

and the transport scattering rate in each band is [41,52]

$$\frac{1}{2\tau_{H,n}} = -\Im \mathrm{m} \Sigma_n^R + \sqrt{\pi} \frac{2\Lambda}{|\tilde{v}_n^{\perp}|} \times \frac{\Im \mathrm{m}[g_n^R W(2\tilde{\varepsilon}\Lambda/|\tilde{v}_n^{\perp}|)]}{\Im \mathrm{m} g_n^R} |\Delta_n(k)|^2. \quad (5)$$

Here R indexes a retarded function, $\Sigma_n = (\hat{\sigma}_n)_{11}$, and $\tilde{v}_n^{\perp}$ is the component of the Fermi velocity normal to $\boldsymbol{H}$.

Results.—We take the e and h FSs to be cylinders of the same size, with $|\tilde{v}_n(\boldsymbol{k})| = v_f$. In the supplementary material we show that our conclusions are robust against modifications of the band structure, and only for the particular case of high curvature of the electronic Fermi surface along the Γ-M line additional care is needed [53]. The unit for the magnetic field is $B_0 = \hbar c/(2e\xi_0^2)$, where $\xi_0 = v_f/2\pi T_{c0}$ is the in-plane coherence length, and T_{c0} is the transition temperature in a pure sample. Highly anisotropic pairing states are affected by the disorder in each band. Hence below we present the results for the purely *intraband*

impurity scattering limit, with the normal state scattering rate, $\Gamma/2\pi T_{c0} = 0.005$, which gives $\lesssim 5\%$ suppression of the transition temperature. We consider strong scatterers, phase shift $\delta = \pi/2$, and checked that smaller δ and moderate interband scattering do not perceptibly change our results. While the BPT method works well for nodal superconductors, its validity in systems with finite minimal gap $\Delta_{\min}$, is restricted to the regime where $v_f/(2\Lambda\Delta_{\min}) \geq 1$ [40]. For $r = 0.45$ in Eq. (1), at the lowest field we consider, $H = 0.02B_0$, this ratio is about 2. Taking $\xi_0 \sim 30$ Å gives $B_0 \simeq 35$ T, so that the fields up to 14 T correspond to $H \lesssim 0.4B_0 \ll H_{c2}$. The last inequality allows for non-self-consistent calculation of the order parameter suppression by the in-plane **H**, which is known to be an excellent approximation [40,51,54].

Figures 2–4 show representative results for C and κ as a function of the field direction at low fields for order parameters $r = 0.45$, 0.55, 1. The panels capture the qualitative behavior across the $T - H$ phase diagram, with only quantitative changes at higher fields and temperatures. The C and κ profiles are slightly shifted vertically for clarity.

Figures 2 and 3 use the gap suggested by the majority of theoretical works, with either minima [$r = 0.45$, Fig. 1(a)] or closely spaced nodes [$r = 0.55$, inset in Fig. 3(d)] in the Γ-M direction, $\phi_0 = 45°$ in our notation. The key feature is the inversion of the specific heat oscillations as the temperature is raised. At the lowest T, H the minima in C/T indeed occur for **H** along the Γ-M line, as expected from the semiclassical theory for zero-energy DOS [37,38,45], but this regime is narrow, and at higher T and H it is the maxima of the C pattern that denote the minima or nodal directions. At low fields the inversion occurs at $0.05 < T/T_{c0} < 0.1$ for deep minima, Fig. 2(a), and at even lower $T/T_{c0} \leq 0.05$ for the nodal case, Fig. 3(a). The same inversion appears for *all* T at fields $H \geq 0.3B_0$, Figs. 2(b) and 3(b). In Ref. [46] the C/T anisotropy was measured at $T/T_c \approx 0.2$. At this temperature the minima in C/T, observed at $\phi_0 = 0, 90$ relative to the crystallographic axes, indicate deep gap minima at $\phi_0 = 45°$ or nodes close to this direction as is evident from comparison with the upper curves in Figs. 2(a) and 2(b) or Figs. 3(a) and 3(b).

In contrast, the experimentally observed pattern is *not consistent* with the nodes along [100] and [010]. Figures 4(a) and 4(b) show minima in the C/T pattern for the field in the nodal direction, $\phi_0 = 0$, only at $T/T_{c0} \leq 0.10$; at higher T additional structure develops, followed by the inversion and the shift of the minima of $C(\phi_0)$ to $\phi_0 = 45°$. This is not what was found in Ref. [46].

Hence possible gap structures are (a) minima along the Γ-M line, or (b) nodes close to this direction. Distinguishing between the two by methods sensitive to the amplitude but not the phase of the gap is not straightforward. While Fig. 3 clearly shows additional features (absent in Fig. 2) at the angles where $|\Delta_e|$ has nodes, these features are washed out with increased temperature. For comparison, κ/T shows nodal features at higher T [panels (c),(d)] than C/T [panels (a),(b)]. With increased scattering this structure smears out and largely vanishes when the nodes are lifted by disorder [55].

Commonly, $\kappa(\phi_0)$ is decomposed into a twofold term due to difference in transport normal and parallel to the vortices [56], and fourfold component due to gap structure [42], $\kappa = \kappa_0 + \kappa_2 \cos 2\phi + \kappa_4 \cos 4\phi$. Both κ_2 and κ_4 change sign in the T-H plane [41,56]. The magnitude of κ_2 is similar in both Fig. 2 and Fig. 3; however, the fourfold κ_4 is much greater for the gap minima than for either nodal scenario. Observation of a large ratio $\kappa_4/\kappa_2 \gtrsim 1$ would indicate minima and not nodes in the gap.

Additional information is needed to distinguish between shallow and deep minima. In Fig. 2 for $r = 0.45$, ($\Delta_{\min}/\Delta_{\max} = 0.1$) the anisotropy in C is $\sim 5\%$ for our choice of the FSs. Setting $r = 0.3$ ($\Delta_{\min}/\Delta_{\max} = 0.4$) we found that this anisotropy drops below 1%, and its inversion occurs at $0.15 \lesssim T/T_{c0} < 0.2$ for similar fields. Also,

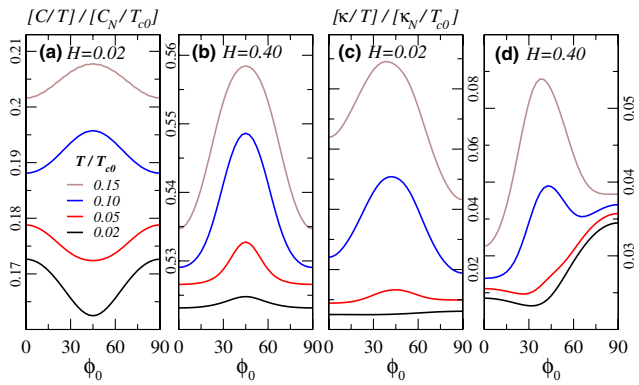

FIG. 2 (color online). The anisotropy of C/T (a),(b) and κ/T (c),(d) for a gap with deep minima along Γ-M line ($\phi_0 = 45°$), as depicted in Fig. 1(a). Except for the low-T, low-H regime, the minima in the gap are marked by the maximum of C. For heat transport, note the same trend, and almost complete absence of the twofold anisotropy in $\kappa(\phi_0)$ at low H and $T \gtrsim 0.05T_{c0}$.

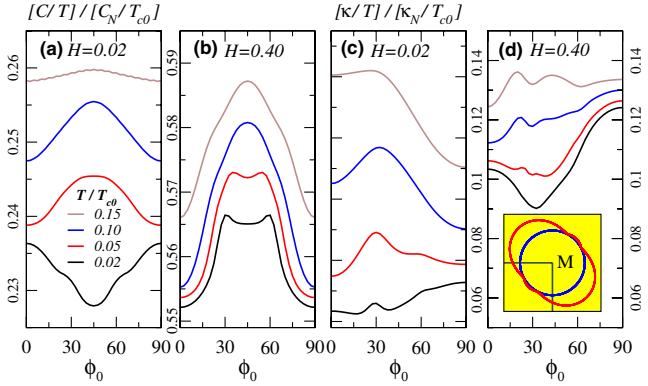

FIG. 3 (color online). The anisotropy of C/T (a),(b) and κ/T (c),(d) for $r = 0.55$, gap with a pair of nodes close to the Γ-M line. The overall behavior is similar to that for deep minima, Fig. 2. The additional structure in C/T for near-nodal directions disappears already at low T, panels (a) and (b); Thermal transport shows additional structure to higher T, and the twofold component is dominant, panels (c) and (d).

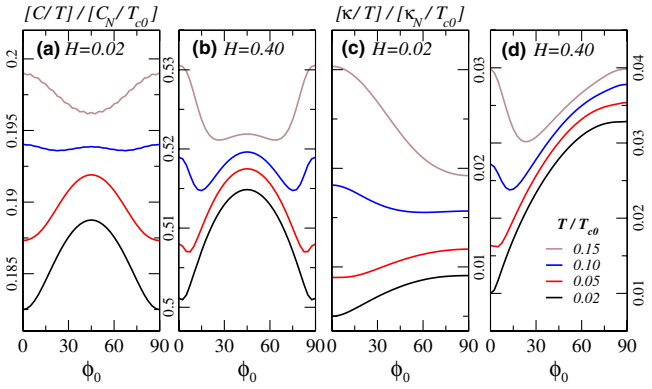

FIG. 4 (color online). Anisotropy of C and κ for $r = 1$, nodes along [100], as in Fig. 1(b). The nodal directions $\phi_0 = 0, 90°$, are marked by minima of C only at $T \lesssim 0.1T_c$. At higher T, H the angle-dependence shows a maximum of C for those directions, as well as additional structure.

above the inversion, the ratio κ_4/κ_2 is much smaller than that for $r = 0.45$. Of course, a larger minimal gap should be evident from measurements even at zero field.

Conclusions.—We developed a framework for the calculation of the anisotropy in the heat capacity and thermal conductivity of two-band superconductors under rotated magnetic field, presented the results for several models of pnictides with anisotropic A_{1g} (''extended s'') gap symmetry, and compared them with an experiment on the Fe(Se,Te) system. We identify either minima ($\Delta_{\min}/\Delta_{\max} < 0.4$) or nodes in the gap on the electronic FS along the Γ-M line, contrary to Ref. [46]. We predict that comparison of the fourfold and twofold term in the anisotropy of thermal transport will help distinguish between the two scenarios. Experiments in a wider T-H range along with the calculations based on realistic FS are clearly forthcoming. Our work lays the foundation for determining the gap structure from these measurements.

We thank A. V. Chubukov, P. J. Hirschfeld, Y. Matsuda, and T. Shibauchi for valuable discussions, and acknowledge partial support from DOE Grant No. DE-FG02-08ER46492 (I. V.) and Aspen Center for Physics.

Note added.—After our manuscript was submitted similar conclusions were reached independently in Ref. [57].

[1] Y. Kamihara *et al.*, J. Am. Chem. Soc. **130**, 3296 (2008).
[2] M. Rotter, M. Tegel, and D. Johrendt, Phys. Rev. Lett. **101**, 107006 (2008).
[3] F.-C. Hsu *et al.*, Proc. Natl. Acad. Sci. U.S.A. **105**, 14262 (2008).
[4] A. Subedi *et al.*, Phys. Rev. B **78**, 134514 (2008).
[5] H. H. Klauss *et al.*, Phys. Rev. Lett. **101**, 077005 (2008).
[6] I. Eremin and A. V. Chubukov, Phys. Rev. B **81**, 024511 (2010).
[7] K. Ishida *et al.*, J. Phys. Soc. Jpn. **78**, 062001 (2009).
[8] I. I. Mazin and J. Schmalian, Physica C (Amsterdam) **469**, 614 (2009).
[9] D. H. Lu *et al.*, Nature (London) **455**, 81 (2008).
[10] C. Liu *et al.*, Physica C (Amsterdam) **469**, 491 (2009).
[11] D. J. Singh, Physica C (Amsterdam) **469**, 418 (2009).
[12] J. G. Analytis *et al.*, Phys. Rev. B **80**, 064507 (2009).
[13] I. I. Mazin *et al.*, Phys. Rev. Lett. **101**, 057003 (2008).
[14] A. Chubukov, D. V. Efremov, and I. Eremin, Phys. Rev. B **78**, 134512 (2008).
[15] F. Wang *et al.*, Phys. Rev. Lett. **102**, 047005 (2009).
[16] K. Kuroki *et al.*, Phys. Rev. Lett. **101**, 087004 (2008).
[17] K. Seo, B. A. Bernevig, and J. Hu, Phys. Rev. Lett. **101**, 206404 (2008).
[18] T. Maier *et al.*, Phys. Rev. B **79**, 224510 (2009).
[19] A. V. Chubukov, M. G. Vavilov, and A. B. Vorontsov, Phys. Rev. B **80**, 140515 (2009).
[20] R. Thomale *et al.*, Phys. Rev. B **80**, 180505 (2009).
[21] S. Graser *et al.*, New J. Phys. **11**, 025016 (2009).
[22] P. Goswami *et al.*, Europhys. Lett. **91**, 37 006 (2010).
[23] H. Ding *et al.*, Europhys. Lett. **83**, 47 001 (2008).
[24] C. Liu *et al.*, Phys. Rev. Lett. **101**, 177005 (2008).
[25] K. Nakayama *et al.*, Europhys. Lett. **85**, 67 002 (2009).
[26] D. V. Evtushinsky *et al.*, Phys. Rev. B **79**, 054517 (2009).
[27] Z. Lin *et al.*, Chin. Phys. Lett. **25**, 4402 (2008).
[28] T. Kondo *et al.*, Phys. Rev. Lett. **101**, 147003 (2008).
[29] K. Kuroki *et al.*, Phys. Rev. B **79**, 224511 (2009).
[30] M. A. Tanatar *et al.*, Phys. Rev. Lett. **104**, 067002 (2010).
[31] J. Fletcher *et al.*, Phys. Rev. Lett. **102**, 147001 (2009).
[32] C. W. Hicks *et al.*, Phys. Rev. Lett. **103**, 127003 (2009).
[33] K. Hashimoto *et al.*, Phys. Rev. B **81**, 220501(R) (2010).
[34] M. Yamashita *et al.*, Phys. Rev. B **80**, 220509(R) (2009).
[35] Y. Nakai *et al.*, Phys. Rev. B **81**, 020503(R) (2010).
[36] M. Bendele *et al.*, Phys. Rev. B **81**, 224520 (2010).
[37] I. Vekhter *et al.*, Phys. Rev. B **59**, R9023 (1999).
[38] I. Vekhter, P. J. Hirschfeld, and E. J. Nicol, Phys. Rev. B **64**, 064513 (2001).
[39] A. Vorontsov and I. Vekhter, Phys. Rev. Lett. **96**, 237001 (2006).
[40] A. Vorontsov and I. Vekhter, Phys. Rev. B **75**, 224501 (2007).
[41] A. Vorontsov and I. Vekhter, Phys. Rev. B **75**, 224502 (2007).
[42] Y. Matsuda *et al.*, J. Phys. Condens. Matter **18**, R705 (2006).
[43] T. Sakakibara *et al.*, J. Phys. Soc. Jpn. **76**, 051004 (2007).
[44] K. An *et al.*, Phys. Rev. Lett. **104**, 037002 (2010).
[45] S. Graser *et al.*, Phys. Rev. B **77**, 180514(R) (2008).
[46] B. Zeng *et al.*, arXiv:1004.2236.
[47] We do not consider here possible gap modulation along the c axis, see S. Graser *et al.*, Phys. Rev. B **81**, 214503 (2010); J. Reid *et al.*, Phys. Rev. B **82**, 064501 (2010).
[48] V. Mishra *et al.*, Phys. Rev. B **80**, 224525 (2009).
[49] A. Houghton and I. Vekhter, Phys. Rev. B **57**, 10831 (1998).
[50] H. Kusunose, Phys. Rev. B **70**, 054509 (2004).
[51] M. Hiragi *et al.*, J. Phys. Soc. Jpn. **79**, 094709 (2010).
[52] I. Vekhter and A. Houghton, Phys. Rev. Lett. **83**, 4626 (1999).
[53] See supplementary material at http://link.aps.org/supplemental/10.1103/PhysRevLett.105.187004.
[54] G. R. Boyd *et al.*, Phys. Rev. B **79**, 064525 (2009).
[55] V. Mishra *et al.*, Phys. Rev. B **79**, 094512 (2009).
[56] K. Maki, Phys. Rev. **158**, 397 (1967).
[57] A. V. Chubukov and I. Eremin, Phys. Rev. B **82**, 060504 (R) (2010).